Journal of Materials Chemistry A

Accepted Manuscript

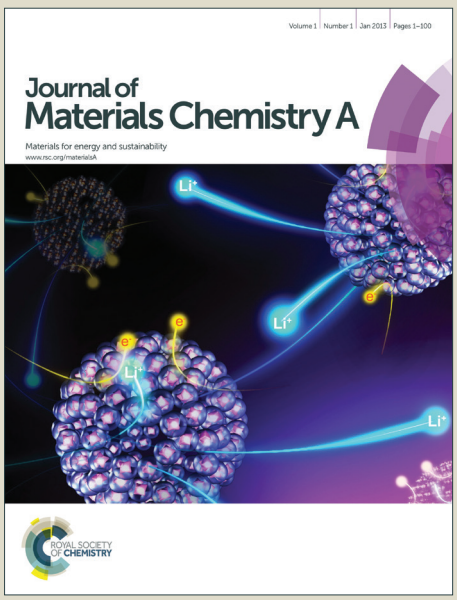

ROYAL SOCIETY OF CHEMISTRY

www.rsc.org/materialsA

Journal Name

RSCPublishing

ARTICLE

Electrochemical Preparation of Metal-organic Framework Films for Fast Detection of Nitro Explosives

Cite this: DOI: 10.1039/xoxxoooooox

Received ooth January 2012,
Accepted ooth January 2012

DOI: 10.1039/xoxxoooooox

www.rsc.org/

Wei-Jin Li, Jian Lü, Shui-Ying Gao, Qiao-Hong Li, Rong Cao*

A facile electrochemical plating method by means of applying voltage onto zinc electrodes in 1,3,5-benzenetricarboxylic acid (H_3BTC) electrolyte has been developed to prepare fluorescent MOF films ($Zn_3(BTC)_2$). Composition of as-prepared MOF films is confirmed by powder X-ray diffraction (PXRD) and surface morphology is examined by scanning electron microscopy (SEM). Voltage and fabrication time are found to be the key parameters for the formation and morphology control of MOF films. Additionally, the as-prepared MOF films, due to their evident fluorescence, are explored for the potential application in detecting nitro explosives at a detection limit as low as 0.5 ppm. The fluorescent MOF films can be further applied to distinguish nitro explosives by varying the solution concentration. Moreover, the MOF films exhibit excellent reusability in consecutive nitro explosive detection reactions. It has been demonstrated that the electrochemical plating method reported here offers a reliable and efficient way to prepare MOF films with controllable morphology for nitro explosive detection.

Introduction

Metal-organic frameworks (MOFs), typically constructed from metal ions and organic linkers, have attracted enormous research attention due to their intriguing structures for coordination chemistry and promising applications in the field of energy and environment, such as catalysis,[1] gas storage and separation,[2] molecular sensing[3] etc.[4] Meanwhile, material scientists have devoted unparallel interest to prepare functional MOF thin films which normally display practical functionalities superior to their bulk crystalline materials.[5] As a result, development of efficient methods and systematic applications of MOF thin films are the main targets confronting a breakthrough in this research area. Of special note, MOF films for molecular sensing is one of the most promising applications due to the controllable and hierarchical features of MOF assembly as well as the fluorescent response of available MOF materials.[5c-f] MOF films have consequently been investigated as optical devices, quartz crystal microbalance based sensors, humidity sensors and so forth.[6]

Detection of nitro explosives is of great interest owing to the ever-increasing concern of environment and homeland security.[7] A large number of fluorescence-based materials, including materials based on fluorescent metal-organic frameworks, have thus been prepared and applied in detection of nitro explosives.[8] For example, fluorescent powder MOF materials or fluorescent spin-coating MOF films were applied as chemical sensors for nitro explosive detection.[9] However, detection application of these chemical materials was plagued either by a struggling recovery and reuse or by uncontrollable surface structures (i.e. microcrystal growth, surface roughness, and morphology).[10] At the same time, detection of nitro explosives using MOF films remained a great challenge due to the extremely strong electron affinity of nitro explosives.[11]

On the other hand, solvothermal synthesis,[12] microwave-assistant heating,[13] and slow solution diffusion[14] have been previously reported to prepare MOF thin films. These synthetic methods are typically multiple-step and time-consuming. Moreover, the substrate surfaces in these synthetic procedures need to be either electro-statically compatible or chemically modified upon pretreatment. Recently, electrochemical preparation of MOF films has been reported based on the HKUST-1 ($[Cu_3(BTC)_2]$; H_3BTC=1,3,5-benzenetricarboxylic

acid) and MOF-5 ($Zn_4O(BDC)_3$, BDC=1,4-benzenedicarboxylate) materials.[15] Electrosynthesis of MOF thin films requires conducting electrodes and ions source, as well as electrolyte of organic linkers for the MOF materials. In such a way, the anode acts directly as support and thus redundant chemical modification or seed coating is avoided. Herein, we propose a facile electrochemical plating method, adapted from the electrochemical patterning, to prepare fluorescent MOF thin films ($Zn_3(BTC)_2$). $Zn_3(BTC)_2$ were found to have identical cell parameters and PXRD to that of $Co_3(BTC)_2$.[16] $Zn_3(BTC)_2$ were found to have identical cell parameters and PXRD to that of $Co_3(BTC)_2$.[16] The crystal structure of the isostructural compounds features zigzag chains of Zn^{2+} ions connected by alternate BTC^{3-} linkers, which are further extended into three-dimensional network *via* hydrogen bonds(Fig.S1). As-prepared MOF films have been thoroughly characterized by a series of physical techniques and tentatively used as sensors for nitro explosive detection thanks to the detectable fluorescence of $Zn_3(BTC)_2$ material. It has been demonstrated that morphology of the MOF films can be well controlled by tuning voltage and fabrication time. The uniform and compact MOF films fabricated at optimized condition (2 V for 40 seconds) have shown fast and efficient detection of nitro explosives with a limit as low as 0.5 ppm. Moreover, the fluorescent MOF films can be applied to distinguish nitro explosives by simply varying the solution concentration. Recycle and reusability of as-prepared MOF films have also been tested based on consecutive detection reactions, in which MOF films remain unchanged and detection efficiency sustains.

Results and discussion

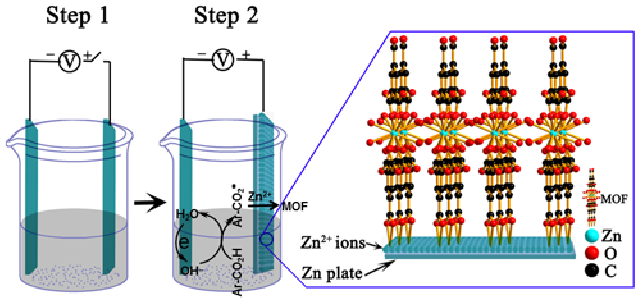

Fig. 1 Schematic view of the preparation procedure of $Zn_3(BTC)_2$ MOF films.

A $Zn_3(BTC)_2$ film was typically prepared by applying a voltage on two electrodes of pure zinc plates in an aqueous solution of H_3BTC and NH_4F. Once electrolysis started, Zn^{2+} ions were produced *via* anodic oxidation on the surface of a zinc plate (anode). Meanwhile, BTC^{3-} anions moved to the anode driven by the electric field. Coordination self-assembly of Zn^{2+} and BTC^{3-} subsequently occurred, which resulted in a $Zn_3(BTC)_2$ thin film deposited on the anodic zinc plate (Fig.1, Fig. S2). Morphology study using SEM showed that rod-shaped MOF microcrystals grew densely on the anodic zinc plate to form a compact and uniform MOF thin film (Fig. 2a and 2b). Thickness of the as-prepared MOF film was at a micron level (Fig. 2b). Experimental powder X-ray diffraction (PXRD) of the MOF film matched well with the PXRD pattern simulated from single crystal data of $Zn_3(BTC)_2$ (Fig. 2c),[16] which confirmed that MOF content deposited on the film was crystalline $Zn_3(BTC)_2$. Moreover, the $Zn_3(BTC)_2$ MOF material has been reported for qualitative detection of organoamines due to its fluorescence.[18] As expected, the $Zn_3(BTC)_2$ MOF films also exhibit detectable blue fluorescence at room temperature in ethanol, which is in agreement with the reported results (Fig. S3), as a heritage of $Zn_3(BTC)_2$ microcrystals.[19]

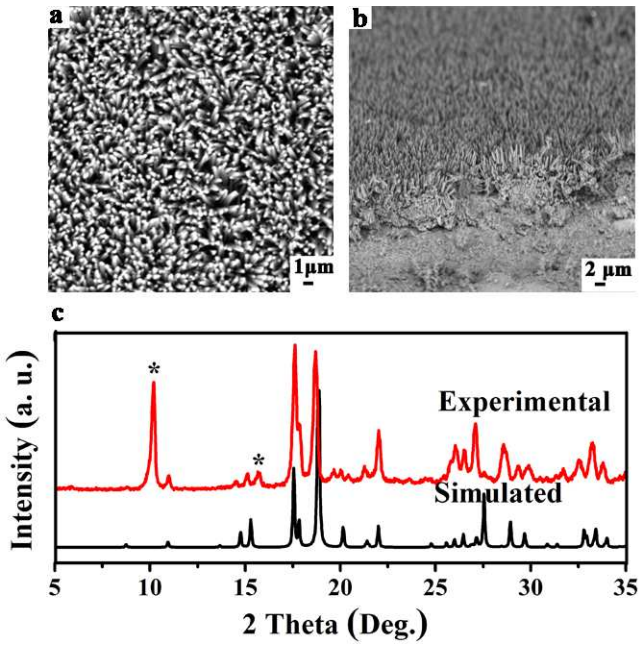

Fig.2 SEM images of (a) top-view and (b) cross-section view at 45°; (c) experimental and simulated powder X-ray diffraction (PXRD) patterns of the MOF film prepared at 2 V for 40 seconds. *Characteristics of $Zn(OH)_2$.[17]

To further study the process of MOF films growth, different voltage was applied to prepare MOF films. The as-prepared MOF films became denser and thicker by increasing the voltage from 0.5 V to 2 V when fabrication time was fixed (Fig. 3, Fig. S4). Corresponding roughness of MOF films are 1.87 μm, 4.55 μm, 14.65 μm and 29.55 μm, respectively, and thickness of MOF films are 1.2 μm, 3.1 μm, 5.1 μm,17.9μm, respectively. At the same time, defect of as-prepared MOF films was reduced with the increase of voltage. It could be rationalized that increasing voltage accelerated the production of Zn^{2+} ions on the surface of zinc anodes as well as the migration of BTC^{3-} to the anodes, which favored the growth of MOF films by offering more nucleation sites and nutrients.[20] Reaction time was also well studied to tune the roughness and thickness of as-prepared MOF films, as well as to monitor the growth of MOF microcrystals on zinc plates (Fig. 4). The roughness and thickness of MOF films prepared at 2 V for 10 seconds was determined to be 3.98 μm and 3.9 μm, respectively. When reaction time was increased, these numbers changed to 7.23 μm and 6.7 μm (for 20 seconds) 16.42 μm and 14.7 μm (for 40 seconds) accordingly, which confirmed the average roughness and thickness were time-dependent. Moreover, it was clear that

the MOF films featured epitaxial growth with time increasing (Fig. S5).

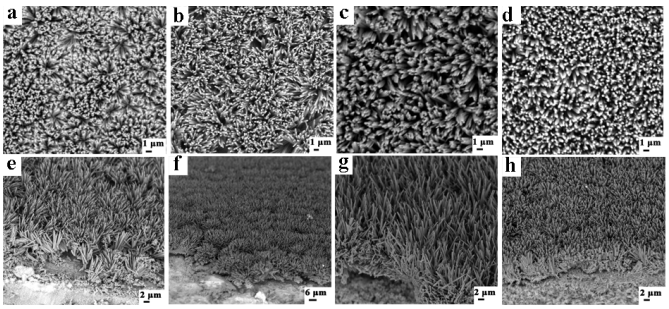

Fig.3 SEM images of MOF films (top-view) prepared at (a) 0.5 V, (b) 1.0 V, (c) 1.5 V, and (d) 2.0 V for 60 seconds, respectively; the corresponding SEM images of cross-section-view at 45° (e, f, g, h).

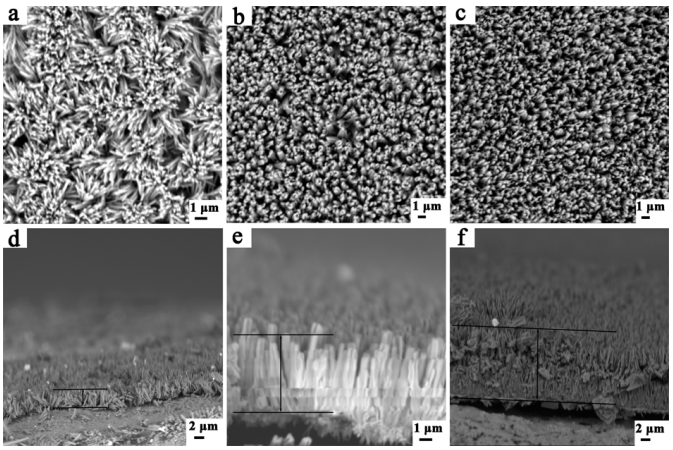

Fig.4 SEM images of MOF films (top-view) prepared at 2 V for 10 seconds (a), 20 seconds (b), 40 seconds (c); the corresponding side-view (d, e, f) SEM images.

The detectable fluorescence and controllable morphology of as-prepared MOF films are promising for their potential usage as sensors. Detection of nitro explosives using as-prepared MOF films has thus been investigated. Nitrobenzene was firstly investigated in ethanol to determine the detection time. As shown in Fig. S6, the MOF films can detect nitrobenzene (100 ppm) after soaking in ethanol for ten seconds. Then, various solvent systems for nitrobenzene (a model nitro explosive) detection, such as ethanol, acetonitrile, cyclohexane, DMF and isopropanol, were investigated to determine the optimized detection condition (original emission spectra see Fig. S7-S11). Fluorescent emission spectra of the MOF films in five solvent systems showed different quenching percentage after soaking for ten seconds (quenching percentage= $(I_0 - I)/I_0 \times 100\%$, I_0 and I are fluorescence intensity of films before and after exposure to the nitro explosives), due to the difference of solvent polarities and their abilities of hydrogen bond formation. The ethanol system gave the highest quenching percentage to the fluorescent MOF films (Fig. S10). Therefore, ethanol was chosen as solvent in following nitro explosive detection reactions of fluorescent MOF films prepared at 2 V for 40 seconds (optimized condition for a compact and uniform film preparation).

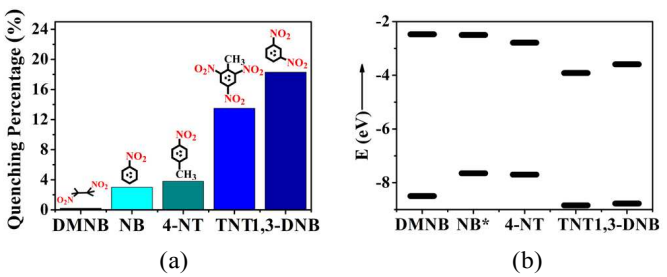

Fig.5 (a) Quenching percentage of MOF films for different nitro explosive detection (0.5 ppm) in ethanol (Excited and monitored at 327 nm and 362 nm, respectively); (b) Theoretical HOMO and LUMO energies for some nitro explosives (Calculated by GAUSS; *reported in literature).

Fluorescence quenching percentage of MOF films for different nitro explosives (at 0.5 ppm) in ethanol was measured after soaking for ten seconds and plotted in Fig. 5a (original emission spectra see Fig. S13-S17). 1,3-dinitrobenzene (1,3-DNB) and 2,4,6-trinitrotoluene (TNT) exhibited significant quenching effect to fluorescent MOF films with quenching percentage of 18.3% and 13.5%, respectively, whereas 2,3-dimethyl-2,3-dinitrobutane (DMNB) showed minor quenching effect as low as 0.21%. Other aromatic nitro explosives, such as 4-nitrotoluene (4-NT) and nitrobenzene (NB), displayed moderate quenching percentage of 3.80% and 2.99%, respectively. For the overall quenching of nitro explosives (200 ppm), 1,3-DNB showed the highest quenching percentage (65.6%), whereas DMNB displayed the lowest quenching percentage of 21.0%. Other nitro explosives, such as TNT, NB and 4-NT, exhibited quenching percentage of 62.2%, 61.9% and 54.1%, respectively. The efficient fluorescence quenching of aromatic nitro explosives can be ascribed to the π-π interactions that favor the interactions between nitro explosives and host materials, which trap effectively the nitro explosives on surfaces, and quenching happens within the system involving electron transfer from the excited MOF microcrystals to electron-deficient nitro aromatic nitro explosives.[21] Unlike the aromatic nitro explosives, however, the weak quenching effect shown by DMNB may be ascribed to the surface self-adsorption that induces electron transfer from the excited $Zn_3(BTC)_2$ microcrystals to the electron-withdrawing DMNB.[21] Generally, the lowest unoccupied molecules orbital (LUMO) energy levels of electron deficient nitro explosives lies lower than the conduction band of the electron rich MOF. Electron from the conduction band transfers to LUMO of nitro explosives upon excitation, leading to the fluorescence quenching.[22] As indicated from theoretical calculations of the LUMO energies,[23] the electron accepting ability of the chosen nitro explosives follows an order of TNT > 1,3-DNB > 4-NT > NB > DMNB (Fig. 5b, Fig. S18).[22a,24] However, the theoretical calculations are not entirely in agreement with the experimental results (for TNT). The discrepancy may be resulted from either the different LUMOs energy levels of nitro explosives to contact with the surface of MOF films or their ability to enter into the spaces among microcrystals on the MOF films, which are related to the substituents and molecular sizes of nitro

explosives.[10c] Moreover, the molecular size of TNT is larger than that of 1,3-DNB (Fig. S19), which restricts TNT molecules to enter into the spaces among the microcrystals on the MOF films. Although TNT has a lower LUMO level than 1,3-DNB according to the theoretical calculations, the electron transfer to TNT was somewhat difficult due to the insufficient diffusion of TNT into MOF films. On the other hand, it is remarkable that the distinguishable detection concentration of various nitro explosives in the current system is as low as 0.5 ppm; meanwhile, the detection of trace amount of nitro explosives is superior to most of other MOF materials for fluorescence quenching based on guest capture (reported detection limit for existing MOF materials in a disperse system or spin-coating MOF films varies from tens to hundreds of ppm) (Fig. S20).[9a,9d,22a,22b,24,25]

Additionally, the concentration-dependent quenching percentage of each nitro explosive was recorded *via* fluorescence quenching titration upon adding different nitro explosives into ethanol solutions where MOF films present (Fig. 6a). It has been found that the on-site fluorescence quenching percentage increases progressively while increasing the concentration of nitro explosives. The quenching efficiency has been analyzed using the Stern-Volmer (SV) equation, $(I_o / I) = K_{sv}[Q] + 1$, where I_o and I are the fluorescence intensity before and after the addition of nitro explosives, respectively, [Q] is the molar concentration of nitro explosives, and K_{sv} is the quenching constant (M^{-1}). The S-V plots for aromatic nitro explosives are nearly linear with K_{sv} of 3.9×10^3 M^{-1} (for 1,3-DNB, regression coefficient, r is 0.940), 7.4×10^3 M^{-1} (for TNT, r=0.988), 5.6×10^3 M^{-1} (for 4-NT, r=0.992), and 7.6×10^3 M^{-1} (for NB, r= 0.988) (Fig. 6b). These results indicate that aromatic nitro explosives are capable of quenching effectively the fluorescence of the as-prepared MOF films. The fluorescence quenching related to aromatic nitro explosives might be either a static or dynamic process.[22a] Absorption spectra verify that it is a dynamic process since collisional quenching only affects the excitation states of the fluorophores, and thus no new characteristic appears to the absorption spectra during the quenching progress (Fig. S21).[26] On the contrary, the non-linear feature of S-V plot for DMNB indicates that the quenching shown by DMNB is not a dynamic process. A possible quenching mechanism for DMNB is based on surface self-adsorption, which induces electron transfer from MOF films to DMNB molecules and leads to a decrease of emission intensity of the host framework.[21] Modified Stern-Volmer equation, $\lg((I_o/I)-1))=\lg Ksv+n\lg[Q]$, is also used to differentiate between dynamic and static quenching, where n is the number of association points between MOF film and nitro explosives, the slope of $\lg(I_o/I-1)$ against lg[Q] defines the association constant.[27] The modified SV plots show that the association points and association constant are 0.222 and 0.212 for 1,3-DNB, 0.328 and 0.138 for TNT, 0.617 and 0.028 for 4-NT, 0.537 and 0.128 for NB (Fig. S22). The results indicate the association constants are small and the association points are below 1.0 which indicates the quenching process is a dynamic process.

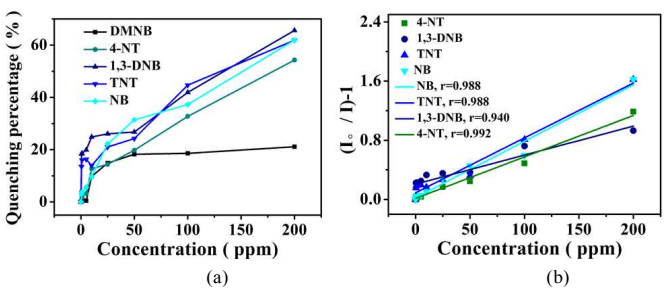

Fig.6 (a) The concentration-dependent quenching percentage of different nitro explosives; (b) Stern-Volmer plots of different nitro explosives (Excited and monitored at 327 nm and 362 nm, respectively).

In order to further understand the mechanism of the quenching processes, different quenching percentages were recorded upon addition of nitro explosives (0.5 ppm) into reaction systems of MOF films with different morphology. Taking 1,3-DNB and DMNB as examples, it was clear that quenching percentage of a nitro explosive vary according to the morphology of MOF films (Fig. 7a). Nonaromatic DMNB showed higher quenching effect to less dense MOF films (prepared at 2 V for 10 seconds and 20 seconds, respectively) than to the denser one (prepared at 2 V for 40 seconds); whereas aromatic nitro explosive 1,3-DNB displayed higher quenching percentage to the denser MOF films than less dense ones (Fig. 7a). Generally, DMNB exhibits lower quenching percentage to denser MOF films, presumably due to the restricted diffusion of nonaromatic DMNB molecules into spaces of MOF microcrystals on the film surface. Nevertheless, in the case of 1,3-DNB, the quenching percentage is mainly dominated by efficient π-π interaction-based surface adsorption, where denser MOF films display enhanced quenching effect favored by available π-π interactions. This observation confirms that distinguishable detection of nitro explosives (non-aromatic versus aromatic ones) can be possible by appropriate choice of MOF thin films with different morphology, which is controllable in this context by reaction conditions (voltage, reaction time etc.).

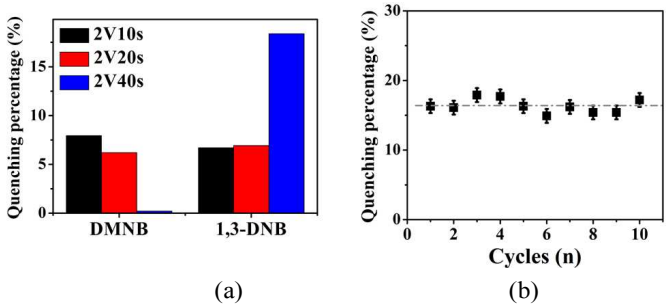

Fig.7 (a) Fluorescence quenching percentage of MOF films with different morphology for DMNB and 1,3-DNB detection; (b) The quenching percentages recorded for recycling experiments in the system of 1,3-DNB (0.5 ppm) and $Zn_3(BTC)_2$ films (ethanol solutions; λ_{ex} = 327 nm, λ_{em}=362 nm).

Durability, recovery and reusability of as-prepared MOF films (prepared at 2 V for 40 seconds) to the best performing quencher, 1,3-DNB, at a concentration of 0.5 ppm were tested for soaking in ethanol for ten seconds. The MOF films showed

equable quenching percentages of 16.4±0.997% during ten consecutive cycles (Fig. 7b). PXRD and FT-IR spectra were collected on the MOF films before and after the detection experiments and showed identical patterns, respectively, which demonstrated MOF microcrystals on the films were able to sustain their structures during the detection experiments (Fig. S23 and S24). SEM images also confirmed that the morphology of the MOF films remained unchanged after detection experiments (Fig. S25). These results indicate that the as-prepared fluorescent MOF films are promising and effective as detective materials for nitro explosives in view of their excellent recovery and reusability.

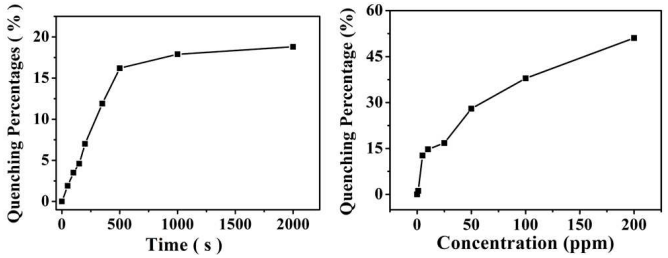

Fig.8 The concentration-dependent quenching percentage of NB in water after soaking for ten seconds. (λ_{ex} = 327 nm, λ_{em}=362 nm)

In order to extend the usage of MOF films in detecting trace nitro explosives, detection of NB vapour using as-prepared MOF films were carried out due to the higher vapour pressure of NB at room temperature. Emission intensity was recorded to monitor the fluorescent quenching of MOF films. The emission intensity of MOF films decreased continuously up to 16.3 % upon exposure to NB vapour for 500 seconds (Fig. 8a; Fig. S26). At the same time, detection of NB in aqueous media was tested in view of the in-filed selective detection of nitro explosives presenting in soil and ground water.[28] The quenching percentage of MOF films for NB (200 ppm) was as high as 51.1% (Fig. 8b; Fig. S27), which is comparable to the number in ethanol system (61.9%). These results suggest that the as-prepared MOF films are promisingly useful for nitro explosive detection at various and practical testing environment.

Conclusions

A series of fluorescent MOF films ($Zn_3(BTC)_2$) with controllable morphology were prepared by a facile electrochemical plating method and consequently used for nitro explosive detection. The plating method has been effective in controlling film morphology via surface engineering, which provides a platform for the assembly and application of fluorescent MOF films. Moreover, the as-prepared MOF films have shown high quenching percentages to aromatic nitro explosives at detection limit as low as 0.5 ppm. The quenching mechanism is mainly dominated by electron transfer in a dynamic quenching process. In this context, the fluorescent MOF films prepared by electrochemical plating can not only detect nitro explosives but also distinguish the nitro explosives by simple adjusting the concentration of quenchers at a practical testing environment, which is superior to the existing MOF materials in a disperse system or MOF films on a substrate by spin-coating for nitro explosive detection.

Acknowledgements

We thank the 973 Program (2011CB932504 and 2012CB821705), National Natural Science Foundation of China (NSFC) (21221001, 21331006 and 21173222), Fujian Key Laboratory of Nanomaterials (2006L2005), and Key Project from the Chinese Academy of Science (CAS) for financial support.

Notes and references

[a] State Key Laboratory of Structural Chemistry, Fujian Institute of Research on the Structure of Mater, Chinese Academy of Science, Fuzhou, 350002, China.
[b] University of Chinese Academy of Science, Beijing, 100049, China.

†Electronic Supplementary Information (ESI) available: general methods, preparation of MOF films, nitro explosive detection and supporting figures. See DOI: 10.1039/b000000x/

1 J. Y. Lee, O. K. Farha, J. Robert, K. A. Scheidt, S. Nguyen, J. T. Hupp, *Chem. Soc. Rev.* **2009**, *38*, 1450-1459.
2 (a) L. J. Murray, M. Dinca, J. R. Long, *Chem. Soc. Rev.* **2009**, *38*, 1294-1314; (b) J. R. Li, J. Sculley, H. C. Zhou, *Chem. Soc. Rev.* **2012**,*112*, 869-932.
3 L. E. Kreno, K. Leong, O. K. Farha, M. Allendorf, R. P. Van Duyne, J. T. Hupp, *Chem. Rev.* **2012**, *112*,1105-1125.
4 H. Ejima, N. Yanai, J. P. Best, M. Sindoro, S. Granick, F. Caruso, *Adv. Mater.* **2013**, *25*, 5767-5771.
5 (a) K. M. L.Taylor-Pashow, J. D. Rocca, Z. Xie, S. Tran, W. Lin, *J.Am.Chem.Soc.* **2009**, *131*, 14261-14263; (b) W.-J. Li, S.-Y. Gao, T.-F. Liu, L.-W. Han, Z.-J. Lin, R. Cao, *Langmuir* **2013**, *29*, 8657-8664; (c) A. Bétard, R. A. Fischer, *Chem. Rev.* **2012**, *112*, 1055-1083; (d) O. Shekhah, J. Liu, R. A. Fischer, C. Wöll, *Chem. Soc. Rev.* **2011**, *40*, 1081-1106; (e) S. Aguado, J. Canivet, D. Farrusseng, *Chem. Commun.* **2010**, *46*, 7999-8001; (f) J. Gascon, F. Kapteijn, *Angew. Chem. Int. Ed.* **2010**, *49*, 1530-1532.
6 D. Bradshaw, A. Garai, J. Huo, *Chem. Soc. Rev.*, **2012**, *41*, 2344-2381.
7 H. Sohn, M. J. Knapp, *Chem. Soc. Rev.* **2009**, *38*, 2543-2555.
8 (a) K. K. Kartha, S. S. Babu, S. Srinivasan, A. Ajayaghosh, *J. Am. Chem. Soc.* **2012**, *134*, 4834-4841; (b) S. W.Thomas III, G. D. Joly, T. M. Swager, *Chem. Rev.* **2007**, *107*, 1339-1386.
9 (a) T. K. Kim, J. H. Lee, D. Moon, H. R. Moon, *Inorg. Chem.* **2013**, *52*, 589-595; (b) S. Barman, J. A. Garg, O. Blacque, K. Venkatesan, H. Berke, *Chem. Commun.* **2012**, *48*, 11127-11129; (c) S. Sivakumar, M. L. Reddy, A. H. Cowley, K. V. Vasudevan, *Dalton Trans.* **2010**, *39*, 776-786; (d) M. Guo, Z. Sun, *J. Mater. Chem.* **2012**, *22*, 15939-15946.

10 (a) J.-S. Yang, T. M. Swager, *J. Am. Chem. Soc.* **1998**, *120*, 11864-11873; (b) J.-S. Yang, T. M. Swager, *J. Am. Chem. Soc.* **1998**, *120*, 5321-5322; (c) A. Lan, K. Li, H. Wu, D. H. Olson, T. J. Emge, W. Ki, M. Hong, J. Li, *Angew. Chem. Int. Ed.* **2009**, *48*, 2334-2338.

11 B. Xu, X. Wu, H. Li, H. Tong, L. Wang, *Macromolecules* **2011**, *44*, 5089-5092.

12 S. Hermes, F. Schröder, R. Chelmowski, C. Wöll, R. A. Fischer, *J. Am. Chem. Soc.* **2005**, *127*, 13744-13745.

13 D. Zacher, O. Shekhah, C. Wöll, and R. A. Fischer, *Chem. Soc. Rev.* **2009**, *38*, 1418-1429.

14 X. H. Bu, F. Liang, Y. S. Li, J. Cravillon, M. Wiebcke, J. Caro, *J. Am. Chem. Soc.* **2009**, *131*, 16000-16001.

15 (a) R. Ameloot, L. Stapper, J. Fransaer, L. Alaerts, B. Sels, D. E. Devos, *Chem. Mater.* **2009**, *21*, 2580-2582; (b) M. Li, M. Dinǎ, *J. Am. Chem. Soc.* **2011**, *133*, 12926-12929

16 O. M. Yaghi, H. Li, T. L. Groy, *J. Am. Chem. Soc.* **1996**, *118*, 9096-9101.

17 We tested that the presence of $Zn(OH)_2$ does not contribute to the fluorescence quenching of nitro explosives even at a gram scale.

18 (a) L. G. Qiu, Z. Q. Li, Y. Wu, W. Wang, T. Xu, X. Jiang, *Chem. Comm.* **2008**, *31*, 3642-3644; (b) X. Q. Zou, G. Z. Zhu, I. J. Hewitt, F. X. Sun, S. L. Qiu, *Dalton Trans.* **2009**, *16*, 3009-3013.

19 (a) X. Shi, G. S. Zhu, Q. R. Fang, G. Wu, G. Tian, R. W. Wang, D. L. Zhang, M. Xue, S. L. Qiu, *Eur. J. Inorg. Chem.* **2004**, 185-191; (b) W. Chen, J. Y. Wang, C. Chen, Q. Yue, H. M. Yuan, J. S. Chen, S. N. Wang, *Inorg. Chem.* **2003**, *42*, 944-946.

20 R. P. Sear, *J. Phys.: Condens. Matter* **2007**, *19*, 033101-033129.

21 L. B. Sun, H. Z. Xing, J. Xu, Z. Q. Liang, J. H. Yu, R. Xu, *Dalton Trans.* **2013**, *42*, 5508-5513.

22 (a) S. S. Nagarkar, B. A. Joarder, K. Chaudhari, S. Mukherjee, S. K. Ghosh, *Angew. Chem. Int. Ed.* **2013**, *52*, 2881-2885; (b) S. R. Zhang, D. Y. Du, J. S. Qin, S. J. Bao, S. L. Li, W. W. He, Y. Q. Lan, P. Shen, Z. M. Su, *Chem. Eur. J.* **2014**, *20*, 3589-3594.

23 M. J. Frisch, G. W. Trucks, H. B. Schlegel, G. E. Scuseria, M. A. Robb, J. R. Cheeseman, J. A. Jr. Montgomery, T. Vreven, K. N. Kudin, J. C. Burant, J. M. Millam, S. S. Iyengar, J. Tomasi, V. Barone, B. Mennucci, M. Cossi, G. Scalmani, N. Rega, G. A. Petersson, H. Nakatsuji, M. Hada, M. Ehara, K. Toyota, R. Fukuda, J. Hasegawa, M. Ishida, T. Nakajima, Y. Honda, O. Kitao, H. Nakai, M. Klene, X. Li, J. E. Knox, H. P. Hratchian, J. B. Cross, V. Bakken, C. Adamo, J. Jaramillo, R. Gomperts, R. E. Stratmann, O. Yazyev, A. J. Austin, R. Cammi, C. Pomelli, J. W. Ochterski, P. Y. Ayala, K. Morokuma, G. A. Voth, P. Salvador, J. J. Dannenberg, V. G. Zakrzewski, S. Dapprich, A. D. Daniels, M. C. Strain, O. Farkas, D. K. Malick, A. D. Rabuck, K. Raghavachari, J. B. Foresman, J. V. Ortiz, Q. Cui, A. G. Baboul, S. Clifford, J. Cioslowski, B. B. Stefanov, G. Liu, A. Liashenko, P. Piskorz, I. Komaromi, R. L. Martin, D. J. Fox, T. Keith, M. A. Al-Laham, C. Y. Peng, A. Nanayakkara, M. Challacombe, P. M. W. Gill, B. Johnson, W. Chen, M. W. Wong, C. Gonzalez, J. A. Pople, *Gaussian 03, revision D.01. Wallingford, CT: Gaussian, Inc.;* **2004**.

24 X. H. Zhou, H. H. Li, H. P. Xiao, L. Li, Q. Zhao, T. Yang, J. L. Zuo, W. Huang, *Dalton Trans.* **2013**, *42*, 5718-5723.

25 (a) T. K. Kim, J. H. Lee, D. Moon, H. R. Moon, *Inorg. Chem.* **2013**, *52*, 589-595; (b) B. Gole, A. K. Bar, P. S. Mukherjee, *Chem. Commun.*, **2011**, *47*, 12137-12139; (c) D. Tian, Y. Li, R. Y. Chen, Z. Chang, G. Y. Wang, X. H. Bu, *J. Mater.* Chem. A, **2014**, *2*, 1465-1470.

26 J. R. Lakowicz, Third edition. *Wiley*, Maryland, **2006**, PP 280-285.

27 H. Zhao, M. Ge, Z. Zhang, W. Wang, G. Wu, *Spectrachim Acta. Part A*, **2006**, *65*, 811-817.

28 S. S. Nagarkar, A. V. Desai, S. K. Ghosh, *Chem. Commun.* **2014**, *50*, 8915-8918.